Antoni RZONCA [1], Karol MAJEK [2]
[1] AGH UNIVERSITY OF SCIENCE AND TECHNOLOGY, 30 Mickiewicza Ave., 30-059 Kraków, Poland
[2] INSTITUTE OF MATHEMATICAL MACHINES, 34 Ludwika Krzywickiego St., 02-078 Warszawa, Poland

Lidarometry as a Variant of Integration of Photogrammetric and Laser Scanning Data

Abstract

This publication aim is discussing the issue of lidarometry – a stereoscopic point cloud display for measurement purposes. The authors state that lidarometry constitutes a valuable variant of integration for photogrammetric and scanning data. A point cloud in lidarometry may be subject to stereoscopic observation and measurement to perform vectorization identically as in photogrammetry. Apart from 3D point cloud display enabled by several programmes in the world, the authors describe the method of synthetic stereograms generation using the artificial image pair sampling, Such solution presents an additional aspect of scanning and photogrammetric data integration and enables thorough analysis of the method. In this publication, the authors describe the genesis and variants of lidarometry. The authors determine the relation of lidarometric measurements accuracy to conventional stereophotogrammetric measurement accuracy. They also provide the optimum point cloud resolution for stereo measurements to terrain pixels size of the measured photograms.

Keywords: lidarometry, data integration, orthoscan, stereoscopy.

1. Introduction

The current development of photogrammetric and scanning methods generates new integration opportunities for these new measurement methods. In practice, there are multiple variations of data integration applied for objects of different sizes and for generations of cartographic products of different parameters and intended use [6, 7, 12]. Also the combined methods, such as point-cloud matching support, are applied [14].

This publication aims at the presentation of the authors own experiences in the field of photogrammetric observation and scanning data measurement methods. Several potential technical solutions for the execution of this measurement method as well as several applications in production will be demonstrated.

Within the research works, accuracy tests for the stereoscopic point height measurements were performed, which enabled determination of the indicated point cloud density against the expected accuracy of digital terrain model measurement, analogical to the one obtained with the photogrammetric stereoscopic model.

2. Lidarometry as an example of measurement technology integration

Stereoscopic observation and measurement result of the point cloud may be specified as lidarometry in analogy to photogrammetry or lidargrammetry [15]. This is a specific variant of applying the photogrammetric tools and method for scanning data measurement purposes. This method has not been commonly applied, however worth discussing in context of data integration and production needs. Its use in the basic variant is feasible only by applying several IT tools in the world. Effective stereoscopic point cloud display and 3D vectorization options are a must. There are two technical solutions known.

The first one is a single display, with exemplary software including DEPHOS Mapper Stereo, DEPHOS LiMonViewer [3], INPHO DTMaster [13], Terrasolid TerraStereo [11].

The second solution consists of displaying simultaneously with the photogrammetric stereoscopic model (DEPHOS Mapper Stereo).

In the first variant, the 3D display of a single point cloud enables display parameters control – including virtual camera parameters and base length, which enables model flexibility regulation and in consequence target accuracy of the stereoscopic measurement. This solution is the case of integration of data originating from two different imaging technologies (stereoscopically measured scanning data i.e. conventional photogrammetric method). The spatial model created by points displayed in the measurement space should be treated as the substitution of one type of data (stereoscopic model created by photogram pair) with data originating from the other parallel technology. In addition, the effect of this scanning data measurement is the generation of data typical for the photogrammetric method. Thus this example is a specific case of integration by substitution.

The case of the simultaneous display of images and cloud seems to be much more interesting both in context of the comprehensive photogrammetric and scanning data integration issue as well as the functional scope. Simultaneous display in technology developed in DEPHOS Software has the option of point cloud or photogrammetric model masking. Proper 3D point cloud display requires the elements of absolute orientation of photograms creating a given photogrammetric model. In such case we may speak about both data integration by substitution – as in the first example – and complete data integration, since data are displayed in the same coordinate system and measured simultaneously [9]. Enabling such measurement implies, among others, correct and analytical data preparation, alignment at the same coordinate system, followed by the correct display. The effect of measurement is data typical for photogrammetry, however originating from the integrated measurement: photogrammetric and LiDAR.

There is also an intermediate solution based on the integration principle, not meeting all the criteria of the lidarometry definition. With the view to the tests described in this publication, the technical assumptions were defined and a tool enabling the generation of synthetic images in central projection at the adopted internal and external orientation parameters were programmed. The images are generated by an algorithm analogical to the sampling algorithm by DEPHOS Software, used for orthoscan generation. This is the authors' own solution, however similar solutions for LiDAR data [2, 10, 15] and radar data exist [4]. The basic difference between stereoscopic point cloud display and this solution consists in the fact that the images are generated via a central projection with indication of the elements of internal orientation of virtual camera and external orientation elements. Such a solution is another example of data integration. Scanning data is processed to photograms able to be observed and measured with the use of each photogrammetric station. This method is not strictly compliant with the lidarometry definition; however, it acts as a valuable complementation for the application of stereoscopy for measurement of data originating from laser scanning, in particular in more comprehensive context of lidarometry i.e. integration of photogrammetric and laser scanning data.

Apart from lidarometry and stereoscopic measurement of synthetic stereogram from the point cloud, there is one more option of photogrammetric and scanning data integration related to 3D cloud point measurement. Stereoscopic measurement should be applied to the point cloud as being the result of dense matching performed e.g. with the use of commercial Agisoft Photoscan software [1]. This complements different options of lidarometry as a data integration tool and acts as a theoretical discussion supported with practical application rather than actual production need.

3. Potential application of lidarometry

Lidarometry may be applied in several production aspects [10].

The first one is a manual measurement with a view to digital terrain model or digital surface model generation. Analogically, it may be used for 3D map measurement. There are cases of projects, in which certain land development elements are well visible in the point cloud, however insufficiently sharp on the images. The example may be the necessary vectorization of the power line structure against the digital surface model to detect potential collisions. Power lines are usually much more visible in the point cloud (laser scanning technology is commonly used for power line inspection), whereas the measurement of digital surface model or its automatic generation may be executed on the basis of scanning or photogrammetric data depending on needs and opportunities.

The other valuable area of lidarometry application is control of digital terrain model or surface model correctness. DTM or DSM observation against the cloud points enables control of their correctness and in the case of terror detection – their edition. There is also the option of complementing the scanning point model with terrain skeleton lines available.

Another application of lidarometry is the abilty to display the results of automatic processes such as matching or dense matching against the stereoscopic model to control and edit the automatically generated GRID or point cloud.

The last production area, which may be successfully executed with the use of lidarometry, is control of data quality and mutual compliance of photogrammetric and scanning data. The practice demonstrates that scanning and photogrammetric data are frequently geometrically inconsistent.

Despite the many advantages of lidarometry, this method has been not commonly applied and only these very few already mentioned tools enabling stereoscopic display and measurements of point clouds are available on the market. There may be many different reasons behind this condition, with the potentially the most important one – separated development of photogrammetry and laser scanning technologies. In production practice, these technologies are frequently integrated, for example in generation of orthophotos with the use of a digital terrain model from the point cloud. However only few companies involved in technological development (in particular IT tools) discovered the capacity of lidarometry, offering the applicable solutions to their customers. Perhaps a significant factor behind such situation is the trend towards increasingly frequent application of automatic method of DTM generation (LiDAR, matching) comparing to manual methods.

4. Description of the assumptions of the performed experiments

Two experiments were performed within the studies on lidarometry.

The first experiment was performed to compare the acquired standard accuracies of the digital terrain model measurements, carried out using the stereoscopic method in 4 different manners. The tests were performed with the use of 4 test fields of different terrain types and development.

The first method is consisted of conventional photogrammetric model measurement. The accuracy of this measurement was considered as the reference accuracy for the remaining 3 manners. The measurement was performed on 4 different test fields in the grid of 50 regular points placed in a distance of 25 m between each other. Each field was measured 5 times to increase the accuracy.

The second manner is consisted in lidarometric point cloud measurement in the same 4 test fields. The cloud was acquired by aerial laser scanning. As in the first case, the cloud was measured using the altitude measurement at the same grid.

The third manner is the point stereoscopic measurement of the point cloud acquired using the Agisoft Photoscan software and dense matching method.

The last, fourth manner is the measurement of synthetic photograms generated on the basis of the point cloud with the research tool constructed for the purposes of lidarometry studies.

For the purposes of the second experiment the same test fields were used. This experiment consisted in comparing the compliance of sufficiently regular point grid measurements found using the following methods:

The first measurement, considered the reference one, was performed on the stereoscopic model in each of 4 test fields.

Then for each of the 4 test fields, 9 sets of point clouds being the subsequent density reduction of the original cloud were generated: from density equal to reference stereogram resolution (0.42 m), each half resolution (0.21 m), to five-fold resolution (2.10 m).

The objective of the second experiment was determination of the impact of point cloud density on lidarometric measurement accuracy with regard to resolution of photograms measured conventionally and the results acquired using such method.

5. Research Tools and Data

5.1. Research Tools

The basic research tool used for stereoscopic measurements in both experiments for all datasets was DEPHOS Mapper Stereo. Data were prepared with the use of CloudCompare software (density reduction of the original point cloud) and Agisoft Photoscan software (generating dense point cloud), whereas after the measurement the Global Mapper (DXF to text format conversion) and calculation sheet was used.

5.2. Research Data

Input data included: image stereogram generated using the DMC method with field resolution of app. 0.42 m and point cloud from the FLIMAP system by Fugro of resolution of app. 20-25 points/sq m i.e. average point distance of 0.20 m.

For both experiments, 4 test fields on the same stereogram within the scanning data coverage of a size covering exactly 50 points each, placed within the regular grid in a distance of 25 m each were selected.

Test field 1 was established at the area of arable lands.

Test field 2 covered the fields and individual single-family buildings as well as afforested area.

Test field 3 covered numerous buildings.

Test field 4 covered the developed area and industrial plant.

For the first experiments the following data sets were prepared:

First set: photogrammetric data – stereogram from DMC camera along with photogrammetric project in the DEPHOS format.

Second set: scanning data in CUBTAB format were cut in a way to ensure that each test field has its own point cloud. In addition the density of them was reduced in the CloudCompare program, thanks to which their density did not exceed the images from DMC camera.

The third set was the cut clouds being the result of dense matching performer in the Agisoft software on the stereogram acquired from DMC camera. Density at the level of density of the a/m images i.e. app. 0.42 m was obtained.

The last, fourth set is a stereogram of synthetic images generated using the own method with the special tool - RzutŚrodkowy2.exe. The artificial images were sampled with the use of the same parameters of internal orientation of camera and elements of external orientation of the photograms corresponding to the model from DMC camera. One may say that the tool made a virtual image of point cloud from the perspective of known projection centers, whereas the image was finally sampled in line with DEPHOS algorithm to generate orthogonal cloud point images, so called orthoscans.

In the case of the second experiment the image stereogram from DMC camera (described above) was used, followed by subsequent density reductions of the input point cloud. Apart from the used point clouds (for 4 test field) of resolution not lower than 0.42 m, the clouds of the following minimum distances between the points (in meters): 0.63, 0.84, 1.05, 1.26, 1.47, 1.68, 1.89 and 2.10. were generated for each of 4 test fields.

6. Empirical research of lidarometric measurement accuracy

6.1. Discussing the first experiment

Within the first experiment, the stereoscopic measurement on the photogrammetric stereoscopic model was performed for each test field, using the lidarometry method on the thinned data acquired from the Flimap system, on dense matching clouds and on synthetic stereograms. There were 32 measurements in total (5 times each for the 4 fields using the photogrammetric method to obtain the mean as reference data and with the remaining methods - 3 times for 4 test fields). Each of 32 measurements covered 50 points. The measurement was performed in such way that the altitudes measured with each method were measured at the same XY points. Then the points were recorded in the calculation sheet, photogrammetric measurements were averaged, altitude differences were calculated (considered as deviations) by subtracting the altitudes measured for the model from the DMC camera from the reference measurement results. In this way, 50 differences for each field and each method were acquired (12 sets in total). For each set the mean, standard deviation and standard deviation of a single result were calculated. The results in tabular and chart form are presented below (Table 1, Fig. 1).

Tab. 1. Arithmetic means of deviations of 3 methods of stereoscopic measurement acquired at 4 test fields including results over 1.5 m

Kind of data	Means Test field 1, m	Means Test field 2, m	Means Test field 3, m	Means Test field 4, m
Lidar	0.14	0.00	0.15	0.01
Dense matching	–0.22	0.17	–0.08	0.16
Synthetic stereo	–0.31	–0.54	–0.46	–0.83

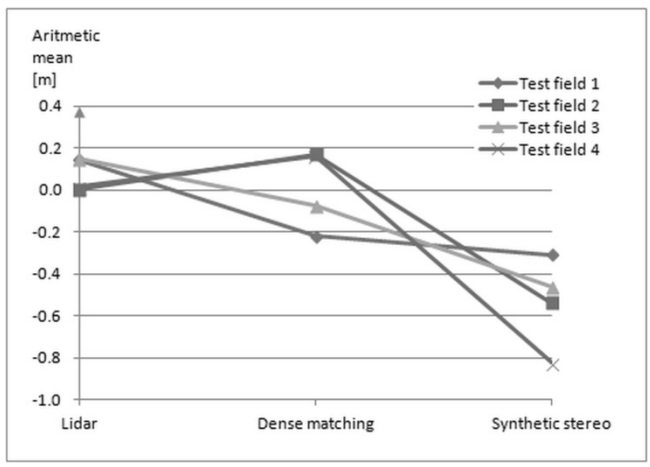

Fig. 1. Linear presentations of aritmetic means of deviations of 3 methods of stereoscopic measurement acquired at 4 test fields including results over 1.5 m

Tab. 2. Standard deviations of means of 3 methods of stereoscopic measurement acquired at 4 test fields including results over 1.5 m

Kind of data	Standard dev. Test field 1, m	Standard dev. Test field 2, m	Standard dev. Test field 3, m	Standard dev. Test field 4, m
Lidar	0.52	0.75	0.90	1.28
Dense matching	0.63	1.79	0.75	1.88
Stereo_synt et	0.53	0.60	1.24	1.56

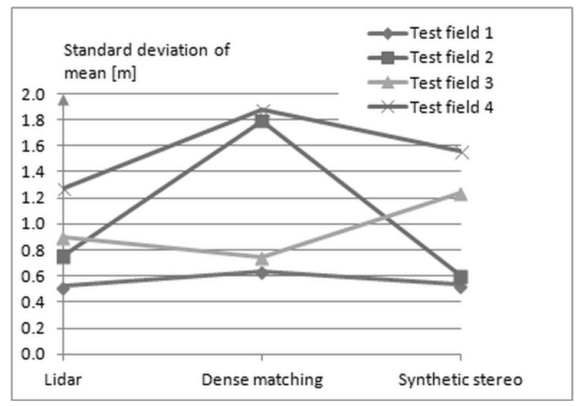

Fig. 2. Linear presentation of standard deviations of means of 3 methods of stereoscopic measurement acquired at 4 test fields including results over 1.5 m

Fig. 1 demonstrates that for the lidarometric measurement on the air point cloud and for the measurements on dense matching cloud for all test fields similar results, oscillating around zero value, were acquired. For these two methods, the deviation means do not exceed 0.5 of field resolution (theoretical altitude measurement error for this case in the baseline ratio of 1:3.5 is app. ±0.7 m). The greater average difference was acquired from measurements on synthetic images, which may be the effect of generally poorer quality of the stereoscopic model generated by this stereogram, resulting in the illusion giving in effect the deviation of systematic nature.

Standard deviations of mean and of the single measurement are of similar nature and values. Therefore only the results of standard deviations of mean (Table 2, Fig. 2) were presented. The lowest values of the standard deviation apply to field 1, covering the arable fields, whereas the greatest values were recorded for field 4 (industrial area), whereas the greatest variability of standard deviations between the measurement methods was recorded for field 2 covering the afforested area. For field 1, the value of 0.7 m was not exceeded for any of the methods, whereas high differences of altitude and ambiguity of certain points of field 4 resulted in exceeding of this value by even 2.5 times.

These results may be summarized as follows. The lowest defects with regard to conventional stereoscopic measurement in photogrammetry are presented by the lidarometric method, whereas the stereo measurements on the matching cloud demonstrates higher distribution due to acquired matching results, in particular in the case of high objects or afforestation. The synthetic stereogram method seems to be promising (when evaluating the variability of standard deviations for different test fields), however requires further enhancements in parameterization in generating the point cloud images. One should notice that there is a number of potential improvements of the method in the field of resampling method, ensuring continuity and sharpness of image as well as known methods of introducing the artificial parallax and modeling its variability depending on accuracy-related expectations [5], [8]. To summarize, this issue seems to be a valuable area of future research.

The means and standard deviations were re-calculated, excluding these deviations, which exceeded 1.5 m and considering theirs errors. It was adopted that the values above two altitude measurement errors could appear in unambiguous points and that such measurement should not be considered when assessing the accuracy of the method.

Tab. 3. Arithmetic means of deviations of 3 methods of stereoscopic measurement acquired at 4 test fields not including results over 1.5 m

Kind of data	Means Test field 1, m	Means Test field 2, m	Means Test field 3, m	Means Test field 4, m
Lidar	0.37	0.03	0.31	0.13
Dense matching	–0.06	–0.22	–0.16	–0.45
Synthetic stereo	–0.09	–0.43	–0.12	–0.38

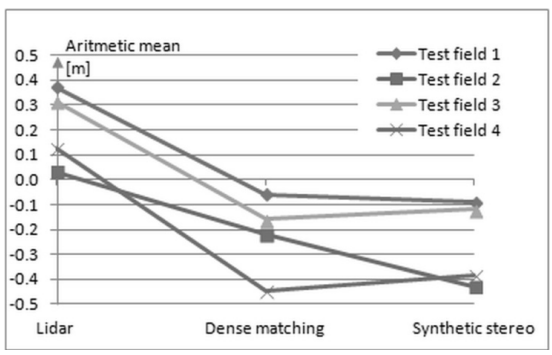

Fig. 3. Linear presentations of arithmetic means of deviations of 3 methods of stereoscopic measurement acquired at 4 test fields not including results over 1.5 m

Tab. 4. Standard deviations of means of 3 methods of stereoscopic measurement acquired at 4 test fields not including results over 1.5 m

Kind of data	Standard dev. Test field 1, m	Standard dev. Test field 2, m	Standard dev. Test field 3, m	Standard dev. Test field 4, m
Lidar	0.41	0.41	0.34	0.41
Dense matching	0.42	0.47	0.47	0.48
Stereo_synt et	0.44	0.46	0.45	0.42

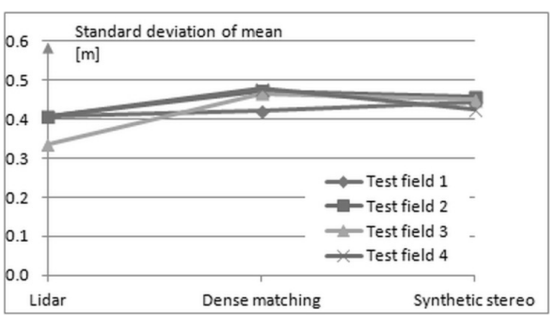

Fig. 4. Linear presentation of standard deviations of means of 3 methods of stereoscopic measurement acquired at 4 test fields not including results over 1.5 m

The acquired results confirmed the interpretation of the results without exclusion of high deviations. Table 3 and Fig. 3 demonstrate regular deviation between the lidarometric measurements and the remaining 3 methods, whereas analysis of Table 4 and Fig. 4 allows for the conclusion that for all test fields in each measurement method the standard deviation of mean show similar values at the level of one field pixel.

6.2. Discussing the second experiment

Within the second set of experiments, 36 measurements for 50 points each were performed: on each of 4 fields 9 lidarometric measurements were made at different point cloud density level (between 0.42 m and 2.10 m). Results of the measurements performed on the photogrammetric method in experiment 1 were used as reference altitudes.

Analogically, as in the first experiment, calculation of means (in (Table 5, Fig. 5) and standard deviations (Table 6, Fig. 6) based on all measurements was followed by exclusion of deviations exceeding 1.5 m. The calculated results are presented below.

Tab. 5. Results of calculated means for different point cloud densities at 4 test fields including results over 1. m

Point cloud resolution, m	Means Test field 1, m	Means Test field 2, m	Means Test field 3, m	Means Test field 4, m
0.42	0.14	0.00	0.15	0.01
0.63	0.14	–0.02	0.24	0.09
0.84	0.09	–0.02	0.17	–0.02
1.05	0.12	0.06	0.24	0.12
1.26	0.22	0.02	0.12	0.11
1.47	0.20	0.00	0.22	0.13
1.68	0.24	0.02	0.00	0.11
1.89	0.21	0.05	0.18	–0.10
2.1	0.22	0.06	0.14	0.03

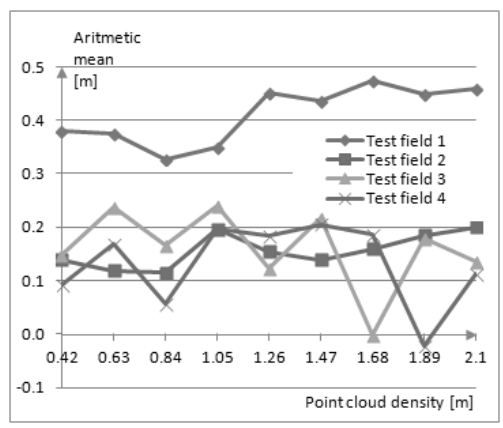

Fig. 5. Variability of calculated means for different point cloud densities at 4 test fields including results over 1.5 m

Tab. 6. Results of calculated standard deviations for different point cloud densities at 4 test fields including results over 1.5 m

Point cloud resolution, m	Standard dev. Test field 1, m	Standard dev. Test field 2, m	Standard dev. Test field 3, m	Standard dev. Test field 4, m
0.42	0.14	0.00	0.15	0.01
0.63	0.14	–0.02	0.24	0.09
0.84	0.09	–0.02	0.17	–0.02
1.05	0.12	0.06	0.24	0.12
1.26	0.22	0.02	0.12	0.11
1.47	0.20	0.00	0.22	0.13
1.68	0.24	0.02	0.00	0.11
1.89	0.21	0.05	0.18	–0.10
2.1	0.22	0.06	0.14	0.03

Then the deviations exceeding 1.5 m were excluded and the means and standard deviations were recalculated.

The second experiment confirmed the trends identified in the first experiment.

The results acquired, with consideration of high altitude differences and the results calculated on the basis of data upon exclusion of deviations exceeding 1.5 m, demonstrate similar trends.

The acquired means (Table 7, Fig. 7) demonstrate random variability and oscillate around zero value and maximally insignificantly exceed the value of a half of field pixel of images from DMC camera, whereas the standard deviations (Table 8, Fig. 8) show the greatest compliance of results for field 1 of non-differentiated land use as well as or the fields 3 and 4 of differentiated land use. Despite density reduction of the measured point cloud from one field pixel of images from the DMC camera to a five-fold field pixel, no results confirming stepwise or linear, significant decrease of measurement compliance were acquired. Minor upward trend appears at low density, however significantly less visible from the expected one. The greatest deviations apply to the area of high differences in altitude (field 4), however without clear upward trend as in the case of field 1 in the arable fields area.

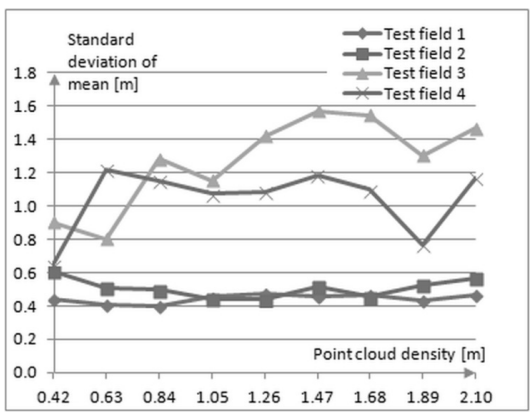

Fig. 6. Curves of changes of the calculated standard deviations for different point cloud densities at 4 test fields including results over 1.5 m

Tab. 7. Results of calculated means for different point cloud densities at 4 test fields not including results over 1.5 m

Point cloud resolution, m	Means Test field 1, m	Means Test field 2, m	Means Test field 3, m	Means Test field 4, m
0.42	0.38	0.20	0.20	0.11
0.63	0.37	0.18	0.20	0.13
0.84	0.33	0.14	0.26	0.02
1.05	0.35	0.22	0.20	0.04
1.26	0.45	0.18	0.25	0.06
1.47	0.44	0.19	0.34	0.14
1.68	0.47	0.18	0.14	0.10
1.89	0.45	0.22	0.28	0.02
2.1	0.46	0.23	0.21	0.07

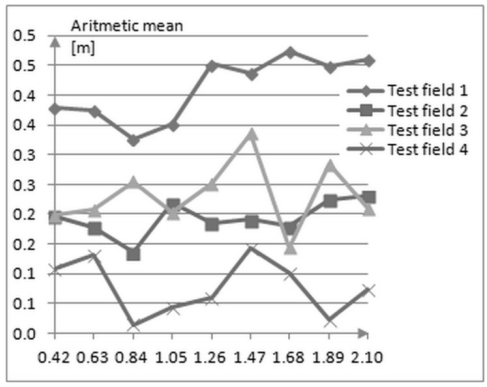

Fig. 7. Variability of the calculated means for different point cloud densities at 4 test fields not including results over 1.5m

Tab. 8. Results of calculated standard deviations for different point cloud densities at 4 test fields not including results over 1.5 m

Point cloud resolution, m	Standard dev. Test field 1, m	Standard dev. Test field 2, m	Standard dev. Test field 3, m	Standard dev. Test field 4, m
0.42	0.44	0.53	0.34	0.44
0.63	0.41	0.42	0.38	0.37
0.84	0.40	0.42	0.35	0.36
1.05	0.46	0.36	0.33	0.37
1.26	0.47	0.36	0.33	0.42
1.47	0.46	0.45	0.33	0.42
1.68	0.47	0.37	0.40	0.44
1.89	0.43	0.45	0.48	0.41
2.1	0.47	0.47	0.44	0.43

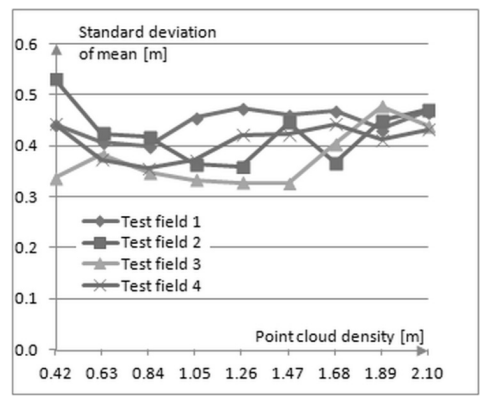

Fig. 8. Calculated standard deviations for different point cloud densities at 4 test fields not including results over 1.5 m

7. Summary and Conclusions

The results of both experiments confirm that lidarometric measurements demonstrate similar results as the measurements made with the use of photogrammetric stereogram.

This result leads to the final conclusion of this publication. We may summarize that the specific nature of lidarometric measurement, consisting in interpolation of the altitude of the measured point on the basis of the surrounding points for the area of insignificant altitude differentiation may be made in thinner cloud, even up to 5 times, or even more. With regard to objects of complex geometry: the lower reduction of point cloud density the more approximate the results to the photogrammetric model.

Preparation of this research work was possible thanks to support provided by the Management Board of DEPHOS Software sp. z o.o., for which the authors express their sincere thanks.

Research is financed under the statutory research at AGH UST no. 11.11.150.949.

8. References

[1] Agisoft, 2016 - http://www.agisoft.com/

[2] Brooks M., Herman B., Flood M.: Lidargrammetry. Direct Exploitation of Stereo Imagery Generated from LiDAR Data. Presentation, 2005.

[3] Dephos Software, Sp. z o.o., 2016 - http://www.dephos.com/software
[4] He X., Balz T., Zhang L., Liao M.: Stereo Radargrammetry in South-East Asia Using Terrasar-X Stripmap Data. ISPRS TC VII Symposium – 100 Years ISPRS, Vienna, Austria. July 5–7, 2010, IAPRS, Vol. XXXVIII, Part 7B, 2012.
[5] Li D. R., Wang M., Gong J. Y.: Principle of seamless stereo orthoimage database and its measurement accuracy analysis. Proceedings of the ISPRS Commission III Symposium, Graz, Austria, pp. 151–156, 2002.
[6] Mitka B., Rzonca A.: Integration of photogrammetric and 3D laser scanning data as a flexible and effective approach to heritage site documentation, International Archives of Photogrammetry, Remote Sensing and Spatial Information Sciences, Vol. XXXVIII-5/W1, Trento 2009.
[7] Nex F., Rinaudo F.: Photogrammetric and LiDAR Integration for the Cultural Heritage Metric Surveys International Archives of Photogrammetry, Remote Sensing and Spatial Information Sciences, Vol. XXXVIII, Part 5 Commission V Symposium, Newcastle upon Tyne, UK, 2010.
[8] Pyka K.: Możliwości wykorzystania stereoortofoto w GIS. The Possibility of Using Stereo-Orthophoto in GIS. Archiwum Fotogrametrii, Kartografii i Teledetekcji, Vol. 23, 2012, pp. 347–354.
[9] Rzonca A.: Integracja danych pozyskiwanych metodami fotogrametrycznymi i skanowania laserowego przy inwentaryzacji obiektów zabytkowych. Integration of photogrammetric and 3D laser scanning data for monumental objects documentation. Monograph, Wydawnictwo AGH, Cracov, 2013.
[10] Smith D.: Lidargrammetry: Using 3D Stereo Photogrammetry for LiDAR Interpretation and Feature Extraction. Presentation. 2013, Washington GIS Conference.
[11] Terrasolid, 2016, http://www.terrasolid.com/products/ terrastereopage.php
[12] Toth C.K., Grejner-Brzezinska D. A.: Complementarity of LiDAR and Stereo Imagery for Enhanced Surface Extraction. International Archives of Photogrammetry and Remote Sensing. Vol. XXXIII, Part B3. Amsterdam, 2000, pp. 897-904.
[13] Trimble, 2016. http://www.trimble.com/Imaging/Inpho.aspx
[14] Wang Z.: Using Stereo Images to Densify LiDAR Data Points at Where Needed, 2012, http://www.isprs.org/proceedings/XXXV/congress/comm3/papers/265.pdf
[15] Ward D.: Lidargrammetry: a look at a new approach for dealing with LiDAR data. Presentation. 2006. http://www.fs.fed.us/eng/rsac/RS2006/presentations/ward.pdf

Received: 12.05.2016 *Paper reviewed* *Accepted: 01.07.2016*

Karol MAJEK, MSc, eng.

Received MSc at Warsaw University of Technology (WUT) Faculty of Mechatronics, specialty: robotics. Currently pursuing PhD at WUT. Working at Modelling and Simulation department at Institute of Mathematical Machines. His main research interests include self driving cars, parallel computing, laser scanning and virtual reality.

e-mail: karolmajek@gmail.com

Antoni RZONCA, PhD

PhD in technical sciences (2008), a graduate of the Faculty of Mining Surveying and Environmental Engineering, AGH in Cracow (2001), specialty: geoinformatics, photogrammetry and remote sensing), adjunct in the Department of Geoinformatics, Photogrammetry and Environmental Remote Sensing, experienced in surveying of historical sites, aerial mission planning and quality control of photogrammetric and scanning data, development of software used in photogrammetry and laser scanning.

e-mail: arz@agh.edu.pl